



## Are maps of nitrate reduction in groundwater altered by climate and land use changes?

Ida Karlsson Seidenfaden<sup>1</sup>, Torben Obel Sonnenborg<sup>1</sup>, Jens Christian Refsgaard<sup>1</sup>, Christen Duus Børgesen<sup>2</sup>, Jørgen Eivind Olesen<sup>2</sup>, Dennis Trolle<sup>3</sup>

<sup>1</sup>Geological Survey of Denmark and Greenland, GEUS, Copenhagen, 1350, Denmark

<sup>2</sup>Aarhus University, Department of Agroecology, Tjele, 8830, Denmark

<sup>3</sup>Aarhus University, Department of Bioscience - Lake Ecology, Silkeborg, 8600, Denmark

*Correspondence to:* Ida K. Seidenfaden, [ika@geus.dk](mailto:ika@geus.dk)

**Abstract.** Nitrate reduction maps have been used routinely in Northern Europe for calculating efficiency of remediation measures and impact on climate change on nitrate leaching and are as such valuable tools for policy analysis and mitigation targeting. Nitrate maps are normally based on output from complex hydrological models, and once generated, are largely assumed constant in time. However, the distribution, magnitude and efficiency of nitrate reduction can not necessarily be considered stationary during changing climate and land use as flow paths, nitrate release timing and their interaction may shift. This study investigates the potential errors when a constant nitrate map is assumed during land use and climate change, both for N-loads and the spatial variation in reduction. For this purpose, a crop and soil model (Daisy) was setup up to provide nitrate input to a distributed hydrological model (MIKE SHE) for an agricultural catchment in Funen, Denmark. Nitrate reduction maps based on an observed dataset of land use and climate were generated and compared to nitrate reduction maps generated for all combinations of four potential land use change scenarios and four future climate model projections. Nitrate reduction maps were found to be more sensitive to changes in climate, leading to reduction map change of up to 10%; while land use changes effects were minor. The study, however, also showed that the reductions maps are products of a range of complex interactions and that the combination of the choices made for selected scenarios, model formulations and assumptions are critical for the resulting span in reduction capability.

### 1 Introduction

Nitrate loads from agricultural areas are recognized to cause harmful impacts on groundwater and surface water resources, including eutrophication in aquatic ecosystems (Diaz and Rosenberg, 2008). This is also the case in the Baltic Sea drainage



basin (Reusch et al., 2018), including Denmark, where nitrate load from agriculture constitutes one of the major water resources management challenges. When assessing the impacts of nitrate leaching from agricultural areas on aquatic ecosystems, the natural removal of nitrate in the groundwater and the surface water must be considered. This removal, often referred to as retention or reduction, takes place via natural biogeochemical reduction processes. It can be expressed as a percentage removal and depending on the actual hydrobiogeochemical conditions the removal may mainly occur in groundwater or in surface water systems such as lakes or wetlands.

In the groundwater zone, nitrate reduction (N-reduction) takes place when nitrate containing water migrates from aerobic to anaerobic conditions (Hansen et al., 2014a; Postma et al., 1991). This transition zone between aerobic and anaerobic conditions is denoted the redox interface. The amount of nitrate reduction occurring in groundwater depends on the flow paths and the depth to the redox interface. In areas with Quaternary sediments characterized by groundwater dominated flow patterns and a relatively shallow redox interface, the N-reduction in groundwater can be the dominant removal process. For example, Højberg et al. (2015) estimated that on average 63% of the nitrate leaching in Denmark is removed by N-reduction in groundwater.

Heterogeneities in geology and drainage systems are responsible for substantial local spatial variations in N-reduction. However the spatial variation of nitrate reduction in the groundwater system has so far only been investigated in a handful of studies (e.g. Højberg et al., 2015; Kunkel et al., 2008; Merz et al., 2009; Wriedt and Rode, 2006). A newer approach for utilizing and illustrating the results and the spatially varying nitrate removal fractions (percentages) are through N-reduction maps (Hansen et al., 2014a). Maps have typically been produced by using complex hydrological models, including simulations of root zone nitrate leaching as well as groundwater and surface flow and transport; and have been applied in several catchments in Denmark and in catchments surrounding the Baltic Sea region (Hansen et al., 2014b; Højberg et al., 2017; Wulff et al., 2014). Hansen et al. (2014a) produced N-reduction maps with a 100 m spatial resolution for a 101 km<sup>2</sup> catchment in Denmark, showing that N-reduction may vary from 20% to 70% between neighbouring agricultural fields located only a couple of hundred meters apart. Similarly, Højberg et al. (2015) and Andersen et al. (2016) estimated very large variations in N-reduction between different regions in Denmark and in the Baltic Sea drainage basin, respectively. When designing and targeting



locations of mitigation measures, it is therefore important to consider how large a fraction of the nitrate leaching from the root zone in specific areas are removed during transport from the root zone to the point of discharge into the sea.

The efficiencies of remediation measures at different locations on N loadings can easily be calculated with N reduction maps, and the measures can be spatially targeted to locations, where the natural removal is relatively small and the effect hence is relatively large (Hansen et al., 2017; Refsgaard et al., 2019). Similarly, N-reduction maps can be used to transform climate change impacts on nitrate leaching from agricultural areas to a catchment response (Olesen et al., 2019). Using N-reduction maps is a much faster method than running complex hydrological simulation models, and is therefore a practical tool for policy analysis (Andersen et al., 2016; Højberg et al., 2015). A severe problem in this respect is, however, that the N-reduction maps are not constant in time but depend on the amount of rainfall and resulting flow pathways. A relevant question is therefore how large errors are made, when N-reduction maps are assumed to be constant in time. No studies have been reported on that issue.

The objectives of the present study are to assess i) how N-reduction maps showing spatially varying nitrate removal fractions in the groundwater zone are affected by changes in climate and land use, and ii) the errors in N loading made by assuming N-reduction maps to be constant. The analyses are performed using a complex hydrological simulation model for a Danish catchment to calculate N-reduction maps for the present conditions as well as for scenarios of climate and land use change.

## 2 Study site

The study site is located in the central part of Denmark on the Island of Funen. It consists of the 486 km<sup>2</sup> upstream part of the Odense River basin, where the Kratholm discharge station marks the outlet (Figure 1). The catchment is drained by a 200 km river network with the outlet located at the Odense Fjord to the northeast. Land use in the area is predominantly agricultural (68%), mainly pig farms followed by dairy and plant production farms (Figure 1). The soil type is dominated by clayey soils (71%) with smaller areas of sand (see Karlsson et al. (2015) and Karlsson et al. (2016) for more information). The discharge station at Kratholm has one of the best nutrient time series in Denmark, providing a long and near-complete data set for nutrient



modelling as well as an extensive water discharge time series (Trolle et al., 2019). The average discharge amounts to 4.4m<sup>3</sup>/s and the load is approximately 14 kg NO<sub>3</sub>-N/ha/year. The geology is mainly a result of previous glaciations like till deposits. Aquifers are generally confined and the phreatic groundwater tables are shallow.

There were 226 measurements of the redox depth in the area. They show a fairly shallow redox interface, where 50% of the 80 measurements have a redox depth less than 4.5 m below terrain, while 90 % of the depths are located in the upper 12.9 meter. An old redox depth map with 1 km resolution, based on measurements and geological interpretation, shows depths between 1 to 5 meters at many locations and between 5 to 15 meters in other locations (Ernstsen et al., 2006). A recent redox depth map of Denmark was created in 2019, where measurements and system variables were used in a machine learning environment to create a detailed 100 meter redox depth map (Koch et al., 2019). This map also indicates that the redox depth in the study area 85 is predominantly shallow with 1-10 meter depth, and very few sites of 10-15 meters depth (Ernstsen et al., 2019).

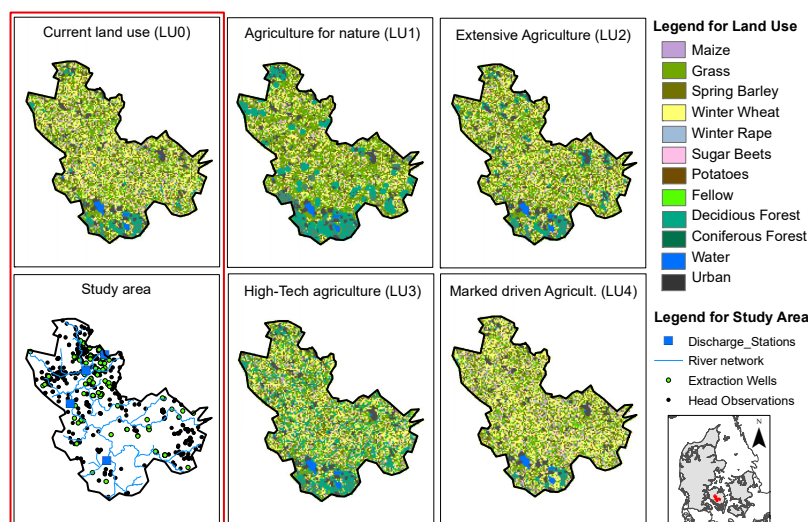


Figure 1: Red square shows the current land use, the river network and water extraction wells and head observations in the 90 catchment: The current land use distribution (LU0) in the study area (Upper left panel) and the river network and location of



observations and extraction wells (Lower left panel). The remaining panels (right and center) shows projected scenarios for land use scenarios LUI-4.

### 3 Methods

#### 95 3.1 Daisy/MIKE SHE setup and calibration

The Daisy-MIKE SHE modeling system is used to describe nitrate transport in the catchment. Daisy is used to quantify leaching of nitrate from the root zone while MIKE SHE is used to simulate the transport and degradation of nitrate in the saturated zone. Both models are forced by the same daily inputs of precipitation, temperature and potential evapotranspiration.

100 Daisy provides a one-dimensional finite difference description of soil-water-crop-atmosphere processes (Abrahamsen and Hansen, 2000; Hansen et al., 1991) where flow is described using Richards' equation and to a minor extent by macro pore flow for loamy soils (Hansen et al., 2012). Nitrate transport is driven by the convection-dispersion algorithm in the soil matrix. Roughly 12,000 1D Daisy columns are setup up in this study to represent unique combinations of soil type, climate, crop rotation and groundwater depth. A more detailed description of the Daisy setup can be found in Karlsson et al. (2016). MIKE  
105 SHE is a fully distributed hydrological model that is built as a modular system with configurable complexity of the different flow compartments (Abbott et al., 1986; Graham and Butts, 2005). To obtain consistency with the flow calculations in Daisy, the present MIKE SHE is also based on a 1D finite difference description of the unsaturated zone using Richards' equation, parameterized by van Genuchten (1980) formulations of the retention curve and the unsaturated hydraulic conductivity curve. A 3D finite difference description of the saturated zone based on Darcy's equation was selected, including a linear reservoir  
110 formulation of tile drainage flow. Drains are specified across the entire catchment as the actual location of tile drains are unknown. Drain flow is however only activated when groundwater level rise above drain level. River flow is described using the MIKE 11 module, where a relatively simple routing method (Muskingum) is used. Additionally, physical formulations for evapotranspiration (Kristensen and Jensen, 1975) and 2D overland flow (DHI, 2019) are selected. The MIKE SHE model was



calibrated using the build-in autocalibration scheme AutoCal (Madsen, 2000). Calibration was carried out against data from  
115 four discharge stations and 455 groundwater wells from the period 2004-2007, see Karlsson et al. (2016) for details.

The one-dimensional Daisy model uses the same climate input as MIKE SHE and calibrated soil parameters were transferred  
from MIKE SHE. Further calibration of the flow compartment of Daisy against observed stream flow sums at the catchment  
outlet was done manually by comparing to accumulated perlocation from all 12,000 columns, following methods proposed by  
120 Allen et al. (1998) and Styczen et al. (2004). Thus, water balance consistency was ensured by calibrating Daisy and MIKE  
SHE such that they produce similar actual evapotranspiration and stream flow for the simulation period.

### 3.2 Nitrate simulations in Daisy

Daisy simulates nitrate leaching for each soil column that represents a unique combination of soil type, climate, crop rotation  
and groundwater depth. Crops are fertilized with mineral nitrogen only and at the crop recommended N rate (2004-2007). N-  
125 input are estimated as daily average nitrate N leaching of the permuted crop rotations simulated for the dominating soil type  
within a 200m x 200 m square grid (Karlsson et al., 2016). Because of the close feedback mechanism between N yields and N  
leaching, the simulated mean N yields were recalibrated to observed annual mean yields on Funen (Statistikbanken, 2015) for  
the dominating soil type for the period 2004-2007 by adjusting the crop parameters. Again following the methodology of Allen  
et al. (1998) and Styczen et al. (2004). N concentrations of yields were extracted from tables on mean N contents for different  
130 crops (Møller et al., 2005).

In the simulations under climate change, the effect of change CO<sub>2</sub> concentration in the atmosphere has an impact on the light  
saturated photosynthesis rate (F<sub>m</sub> parameter), which is not included in the Daisy crop model code. In order to deal with this  
mechanism, the procedure described in Børgesen and Olesen (2011) was adopted.

### 135 3.3 The Nitrate model

The nitrate model is constructed by combining the two models, Daisy and MIKE SHE. Daily values of nitrate flux from Daisy  
serves as input to MIKE SHE, where nitrate transport is simulated by converting nitrate input to particles using the particle-



tracking module. Each time the accumulated input of nitrate reach 0.5 kg N, a particle is released from the water table and is allowed to follow the groundwater flow. If the particle penetrates the redox interface, the nitrate is assumed to be removed completely and instantaneously by denitrification. Remaining particles will emerge in discharge zones typically located in stream valleys and leave the catchment at the river outlet (Kratholm station). The nitrate arrival percentage (NAP) is found as the accumulated amount of N leaving the catchment divided by the amount released at the water table. The nitrate model was calibrated by adjusting the depth to the redox interface (see section 0) until an acceptable match to the observed NAP was obtained. A more detailed analysis and description of the nitrate transport method can be found in Hansen et al. (2014b).

### 145 **3.4 Estimation of depth to redox interface**

The redox interface depth for each cell in MIKE SHE is determined using a five step method developed by Hansen et al. (2014a). The method is based on the assumption that the present location of the redox interface is a result of the cumulative oxygen percolation through the soil column since the last ice age in the Holocene 11,700 BP.

150 The redox interface is assumed to have been at ground level at the end of the glaciation and to have migrated downwards by an unknown number of millimeters per yearly recharge. Following the procedure of Hansen et al. (2014a), first step is therefore to find the average yearly recharge, by running a model simulation without anthropogenic influences (abstraction and tile drainage). In the second step, the different redox capacities in soils are accounted for, where the capacity of sandy soils are multiplied with a factor of three compared to value specified for the clayey soil types applying the classification from Børgesen et al. (2013) and Greve et al. (2007). The third step generates the redox interface expressed through equation (3):

$$Redoxdepth_i = flux_i * f + min.redoxdepth$$

where  $Redoxdepth_i$  is the redox depth (m) calculated at each grid (i),  $flux_i$  is the groundwater recharge (m/yr) which is multiplied by the migration constant  $f$  (yr) (Hansen et al., 2014a). The upper part of the unsaturated zone is assumed to have no redox capacity due to very fast air diffusion, which is accounted for using a minimum redox depth,  $min.redoxdepth$  (m).

160 To account for unrealistically high values of the redox depth, a maximum redox depth is also estimated based on the principles of Hansen et al. (2014).



Hereby, the spatially distributed redox interface is quantified and incorporated into the MIKE SHE nitrate model (step four) and the location of the redox depth is then calibrated by adjusting  $f$  and  $\text{min.redoxdepth}$  to obtain the observed NAP (step five),  
165 and subsequently compared with the measured redox depth in boreholes.

### 3.5 Estimation of reduction map and map correction

The reduction map quantifies the nitrate reduction potential for each model grid (Hansen et al., 2014a). The number of representative particles released at each cell that is subsequently reduced is divided by the total number of particles released. The reduction map is therefore based on results from the nitrate model that is run with the calibrated redox interface. In the  
170 reduction map, a grid with the value of 100% indicates that all particles released in the cell are subsequently reduced, while a value of 50% indicates that half of all particles (nitrate) reaches surface waters unreduced. Therefore, it provides valuable information on what the environmental impact in terms of nitrate loading of farming practices are for specific parts of the landscape.

175 Unfortunately, during the release of particles in the MIKE SHE model, numerical issues occasionally cause some particles to get stuck in the unsaturated zone. The actual fate of these particles (reduced/non-reduced) are therefore unknown. At an early stage the assumption was made that the captured particles, if they had moved correctly through the system, would be subject to a fate similar to the non-captured particles, i.e. that the relationship between reduced/non-reduced was the same. If this assumption is valid the calculation of a direct arrival percentage (meaning a reduction map multiplied with the nitrate input)  
180 should give the same arrival percentage as calculated based on the more complex particle arrival count excluding these captured particles. However, this was unfortunately found not always to be the case.

As it was not possible to correct this numerical error in the model code, or in any other way account for this model limitation, a correction scheme was introduced. The correction factor uses a simple linear equation, where the correction factor is manually  
185 fitted so that the direct arrival percentage matches the particle arrival percentage. These corrections are done individually for all reduction maps, and the correction causes a change in the reduction in the range of -7% to 9% with a mean of 2%.





### 3.6 Climate and land use scenarios

The hydrological model was forced by 16 scenarios for future climate and land use. One emission scenario, the IPCC AR4 SRES A1B scenario (Nakicenovic et al., 2000) where chosen as the basis for this study. Since the study was conducted newer generations of emission scenarios have been developed by the IPCC (van Vuuren et al., 2011), known as the Representative Concentration Pathways (RCPs); the A1B scenario is generally comparable to the RCP6.0-emission scenario (medium scenario).

In this study, realizations from four climate model combinations, GCM-RCM couplings, were selected from the ENSEMBLES project (Hewitt and Griggs, 2004), where results from the period 2080-2099 were extracted and used as input to the hydrological model. Data from both this period and the reference period, 1990-2009, were bias-corrected using the DBS method, which is a direct method that preserves the dynamics and non-stationary nature of the raw climate model results (Seaby et al., 2013). The four selected realizations represent a wet, +19% in precipitation (ECHAM-HIRHAM5), a dry, -11% decrease in precipitation (ARPEGE—RM5.1), a warm, +3.4 °C temperature increase (HadCM3-HadRM3) and a median model, +10% in precipitation and +2.1 °C in temperature (ECHAM5-RCA3). The change factors can be seen in Table 1. Both climate models and bias-corrections are described in more detail in Karlsson et al. (2016).

Season mean	Climate model	CHANGE FACTOR		
		Precipitation	Temperature	RefET
Annual	ARPEGE—RM5.1	0.88	2.14	1.12
	ECHAM5—HIRHAM5	1.28	2.08	0.94
	ECHAM5—RCA3	1.17	2.22	0.94
	HadCM3—HadRM3	1.00	3.72	1.19
Fall	ARPEGE—RM5.2	0.74	2.05	1.23
	ECHAM5—HIRHAM6	1.20	2.45	1.02
	ECHAM5—RCA4	1.18	2.35	0.98
	HadCM3—HadRM4	0.93	4.11	1.33
Winter	ARPEGE—RM5.3	1.18	2.40	1.24
	ECHAM5—HIRHAM7	1.30	2.65	1.22
	ECHAM5—RCA5	1.30	2.64	1.03
	HadCM3—HadRM5	1.31	4.19	1.57



Spring	ARPEGE–RM5.4	0.95	1.83	1.03
	ECHAM5–HIRHAM8	1.33	1.72	0.92
	ECHAM5–RCA6	1.18	2.03	0.88
	HadCM3–HadRM6	1.02	3.24	1.07
Summer	ARPEGE–RM5.5	0.67	2.29	1.14
	ECHAM5–HIRHAM9	1.32	1.50	0.90
	ECHAM5–RCA7	1.02	1.88	0.96
	HadCM3–HadRM7	0.78	3.36	1.19

**Table 1: Change factor for the four climate model combinations for precipitation (multiplicative), temperature (°C - additive) and**

205 **reference evapotranspiration (multiplicative)**

The four climate model realizations were combined with four land use scenarios that describe agricultural management in the period 2080-2099 as: LU1: “Agriculture for nature”, where the agricultural area is reduced to 40% of the land area through afforestation and increasing grass areas and fertilization rates are generally reduced (-40%); LU2: “Extensive agriculture” with  
 210 a small 3% point reduction in agricultural area resulting in 64% farmland; however, some of the intensive farm types (with high fertilization rates) are converted to less intensive farm types with less fertilization (total change of -60%); LU3: “Hightech agriculture”, also with a small decrease in agricultural area of 3%, but with a productivity of crops that is assumed to increase, resulting in an insignificant change in the needed fertilizer inputs (0%); LU4: “Market driven agriculture”, where forest and  
 215 some extensive farm types are converted into intensive farming resulting in an agricultural area of 70%. At the same time, fertilization rates are increased to reach maximum production (+20%). More information on the land use scenarios can be found in Olesen et al. (2014) and Karlsson et al. (2016).

All 16 combinations of future climate projections and land use were specified as input to the hydrological model and compared to the climate model results found for the reference period 1990-2009 using the same land use scenarios, resulting in 32  
 220 scenarios. Additionally, the model was run with observed climate for the period 1990-2009 (using observed land use and the four land use scenarios) and observed land use for the period 1990-2009 (combined with the observed climate and results from the four climate models). Hence, a total of 50 model simulations were analyzed. In this paper the following terminology is used:



- Observational period: Results from a hydrological model and the rootzone model Daisy run forced with  
225 observational data in the period 1990-2009. This period covers both the calibration period (2004-2007) and  
validation periods (2000-2003 and 2008-2009), all of which are driven by observational data.
- Reference period: This period is used to describe specifically the climate model driven hydrological results from the  
period 1990-2009.
- Future period: The future scenario refers to climate model forced runs for the period 2088-2099.
- 230 • Baseline: The term baseline refers to results from the specific model run combination (no. 1), where current land  
use scenario (LU0) is combined with the observational climate data.

## 4 Results

### 4.1 DAISY and MIKE SHE model evaluation

A detailed presentation and evaluation of the water quantity performance of MIKE SHE and DAISY, have previously been  
235 described in Karlsson et al. (2014). MIKE SHE was reported to have good performance in the calibration (and validation  
periods) with water balance error of 3% (6-10%); and RMSE value of 1.5 m<sup>2</sup>/s (1.2-1.5 m<sup>2</sup>/s). Due to the complicated setup  
with manual simultaneous calibration of more than 12.000 1D DAISY models, the water balance performance of the DAISY  
model was reported to be somewhat poorer with water balance errors of 16% in the calibration period and 3- 23% in the  
validation periods.

240 The results from the subsequent manual calibration of the nitrate leaching in DAISY using the N yields for the region, can be  
seen in Table 2. For all the crops in the region the DAISY model is able to reproduce the observed harvested N within a margin  
of 0-5 kg harvested N/ha. The DAISY model is therefore able to represent the observed trends in nitrate yields to a satisfactory  
level on catchment scale.



245 **Table 2: Observed and simulated harvested N in kg N/ha for the crop type on Funen during the calibration period 2004-2007. Grain type crops are stated as harvested N in the grain, while the remaining crops are calculated as total harvested dry matter.**

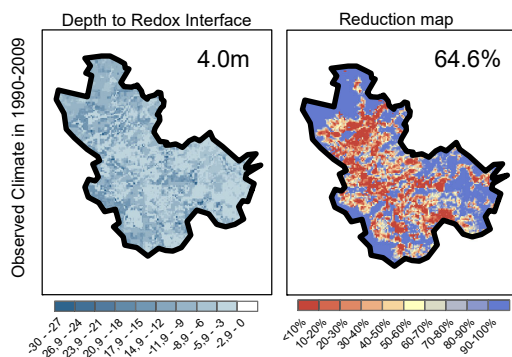
Crop	Observed harvested kg N/ha	Simulated harvested kg N/ha
Spring barley	101	102
Winter wheat	122	124
Winter rape	105	107
Silage maize	151	152
Grass in rotation	258	259
Grass permanent	78	83
Sugar beets	179	179
Grain maize	No data	-

#### 4.2 Baseline nitrate reduction map

The observed nitrate arrival percentage (NAP) of the catchment was estimated to 35-39%. The span is a result of the choice of  
250 time period; however, a NAP of 37% was selected as the final calibration target. Several different combinations of the migration constant ( $f$ ) and the minimum redox depth (min.redoxdepth) result in a NAP of 37%. To select the most appropriate combination, the cumulative distribution of the resulting redox depth of a given parameter combination is plotted against the distribution of observed redox depths. The observed redox depth is both compared to the simulated values at the actual point of observational measurement as well as to the total fractional distribution of the whole catchment (not shown). Based on this  
255 analysis the best combination with the correct NAP was found to be  $f=0.01\text{yr}$  and  $\text{min.redoxdepth}=3\text{m}$ . Figure 2 (left) shows the resulting depth to the redox interface for this combination. Generally, the depth to the redox interface is fairly shallow,



with a mean depth of 4.0 meters (standard deviation of 5.6 m). This corresponds fairly well with the previously reported redox depth (Koch et al., 2019).



260 **Figure 2: Left – Resulting depth to redox interface after calibration. Right - Nitrate reduction potential maps for the baseline scenario (Land use 0/observed climate), showing the fraction of the leached nitrate that are reduced for each grid. The number in the upper right corner of each panel is the average across all grids.**

The baseline reduction map was generated based on the nitrate input from the DAISY model for the present period and the current land use (Figure 2, right). The mean N reduction fraction in the catchment is 65% with a standard deviation of 38%  
265 points. The spatial distribution on the map shows high reduction potentials in the uplands at the border of the model, likely where infiltrating water has a longer travel path to the river, and in areas where the redox interface is shallow. Lower reduction potential is seen in the areas near the stream network and lowland areas with deep redox interface.

#### 4.3 Reference and future nitrate reduction map

Utilizing the different nitrate input from the land use/climate model scenarios, 45 nitrate models (observational, reference and  
270 future, Table 3) were run with the calibrated redox interface. The depth to the redox interface is ergo assumed to be constant in time and is not updated for each scenario. This assumption is acceptable because of the slow migration of the interface, where the migration constant predicts one meters downward movement every 100 years. Following the procedure described in section 0, this generates 45 nitrate reduction potential maps. The statistics for all 45 reduction potential maps is shown in



Table 4, and a selection of these reduction maps can be seen in Figure 3. In the top row in Figure 3, the observed climate is  
275 used, changing only the land use (scenarios 2-5). In the bottom row the present land use (LU0) is used, while using future  
climate projected by the four climate models (scenarios 26, 31, 36 and 41).



Period	Climate	Land use (LU) scenario				
		Baseline	Agriculture for nature	Extensive agriculture	High-tech agriculture	Market driven agriculture
Control period, 1990-2009	Obs. Climate	1	2	3	4	5
	ECHAM5-HIRHAM5	6	7	8	9	10
	ECHAM5-RCA3	11	12	13	14	15
	ARPEGE-RM5.1	16	17	18	19	20
	HadCM3-HadRM3	21	22	23	24	25
Future period, 2080-2099	ECHAM5-HIRHAM5	26	27	28	29	30
	ECHAM5-RCA3	31	32	33	34	35
	ARPEGE-RM5.1	36	37	38	39	40
	HadCM3-HadRM3	41	42	43	44	45

Table 3: Land use and climate scenario matrix showing the scenario numbers.

280

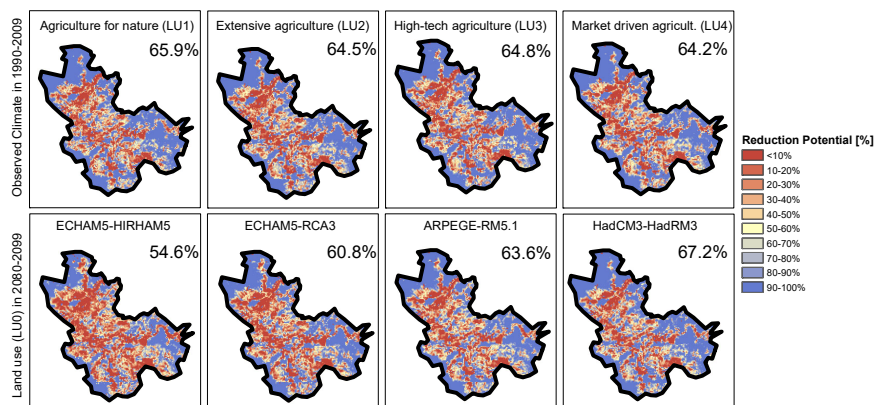


Figure 3: Nitrate reduction potential maps for four land use scenarios (LU1-4) in the observational period (top row) and four climate scenarios (LU0) for the future climate (bottom row), showing the fraction of the added nitrate that is reduced for each grid.

285



Period	Climate input	Land use				
		Baseline	LU1	LU2	LU3	LU4
Control period (1990-2009)	Obs. Climate	0.65 (0.38)	0.66 (0.38)	0.65 (0.38)	0.65 (0.38)	0.64 (0.37)
	ECHAM5-HIRHAM5	0.62 (0.38)	0.63 (0.38)	0.62 (0.38)	0.62 (0.38)	0.62 (0.38)
	ECHAM5-RCA3	0.65 (0.37)	0.66 (0.37)	0.65 (0.37)	0.65 (0.37)	0.64 (0.37)
	ARPEGE-RM5.1	0.69 (0.36)	0.70 (0.36)	0.69 (0.36)	0.68 (0.37)	0.68 (0.36)
	HadCM3-HadRM3	0.63 (0.38)	0.64 (0.38)	0.61 (0.38)	0.63 (0.38)	0.62 (0.38)
Far future (2080-2099)	ECHAM5-HIRHAM5	0.55 (0.38)	0.55 (0.39)	0.55 (0.38)	0.55 (0.39)	0.54 (0.38)
	ECHAM5-RCA3	0.61 (0.38)	0.62 (0.39)	0.61 (0.38)	0.61 (0.39)	0.60 (0.38)
	ARPEGE-RM5.1	0.64 (0.37)	0.64 (0.38)	0.64 (0.37)	0.63 (0.37)	0.63 (0.37)
	HadCM3-HadRM3	0.67 (0.37)	0.68 (0.37)	0.67 (0.37)	0.66 (0.37)	0.65 (0.37)

**Table 4: Mean and standard deviation (in brackets) of nitrate reduction potential maps (proportion of nitrate N reduced).**

All scenarios show similar patterns of reduction zones with high and low removal fractions when compared to the baseline scenario map (Figure 2). However, although the general pattern of the reduction maps is comparable, there are spatial differences between the maps. The redox depth remains constant and all nitrate crossing this interface are assumed to be reduced, regardless of amount. Therefore, the reason for these changes in the nitrate reduction potential map results from changes in the flow path and/or changes in N-input from Daisy, reflected in differences between drain/interflow versus groundwater flow to streams, and timing of nitrate release from the root zone.

To investigate to what degree land use changes and climate change affect the reduction map, the difference between these scenarios and the reference scenario is shown in Figure 4.



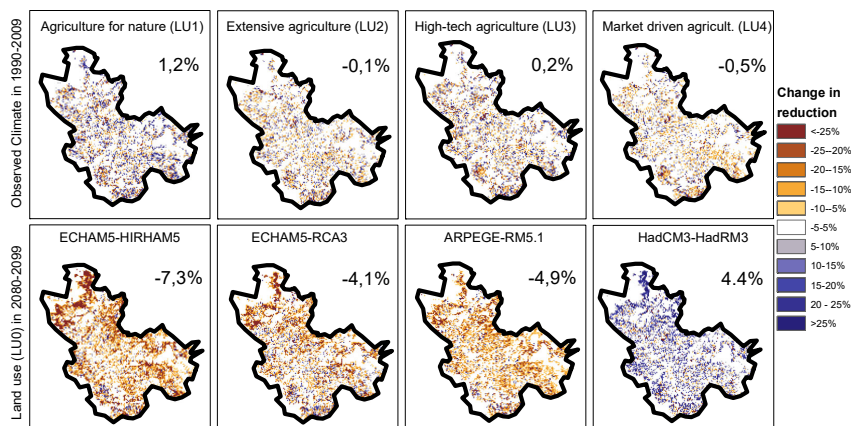
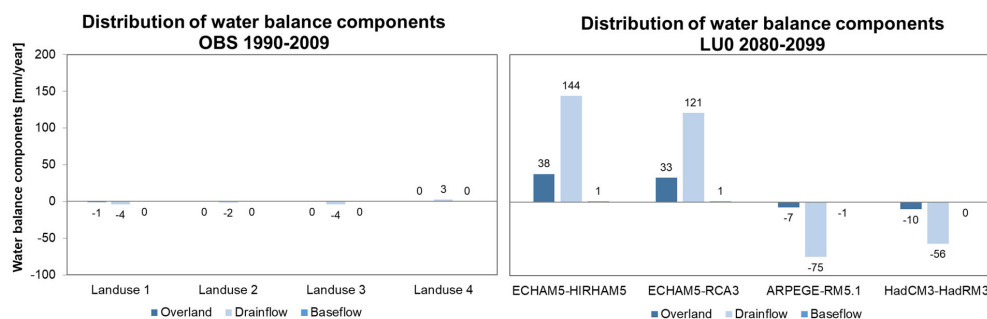


Figure 4: Difference in nitrate reduction potential maps between: Top row - Four land use scenarios LU1-4 (Scenario 2-5) and the baseline scenario with land use 0 (Scenario 1). Bottom row: The four future climate model scenarios (scenarios 26, 31, 36, 41) and the reduction maps for the corresponding climate model reference period (scenarios 6, 11, 16, 21) all for land use 0.

#### 4.4 Impact of land use change on reduction maps

To investigate the impact of land use change on the reduction maps, only land use is changed while climate remains constant. The water balance of the models, and hence the groundwater level and water flow paths, are affected mainly by a possible change in evapotranspiration that is introduced with new crop rotation systems and vegetation types. Drains are still present in the entire catchment regardless of land use and are only active when they are required (submerged below the groundwater table). At the same time, the land use changes result in a nitrate input distribution and timing that may differ from the current land use (LU0). The changes are minor and give both higher and lower reduction potential, depending on changes in land use and vegetation for the individual grids (Figure 4, top row).

The changes in the average catchment water flow components as a result of land use change is shown in Figure 5, left. This shows the change of each component, drain flow, overland flow and base flow, when changing from a scenario run with land use 0 to the scenarios with land use 1-4. These changes minor for the overall water balance on the catchment scale for all land use change scenarios (Figure 5, left).



315

**Figure 5: The change in the water balance components in mm/year caused by changes in land use and climate change. Left – The difference for the four land use scenarios LU1-4 (Scenario 2-5) and the baseline scenario with land use 0 (scenario 1). Right: The difference between the four future climate model scenarios (scenarios 26, 31, 36, 41) and the corresponding climate model reference period (scenarios 6, 11, 16, 21) all for land use 0 (modified from Karlsson et al. (2016)).**

320 The drain flow component is a primary conductor for non-reduced nitrate, because it represents fast and shallow flows above the redox interface. It is therefore relevant to look at the spatial distribution of the changes in drain flow for the scenarios. While the bias corrections ensure that the climate models reproduce the overall mean and variances of the observed climate, they do not necessarily ensure consistency in the temporal structure of precipitation. Hence, the overall net precipitation may change slightly across the climate models, and we have therefore plotted the change in drain flow fraction (Figure 6), defined as the drain flow divided by net precipitation, instead of the drain flow component itself. As for the changes in the reduction map (Figure 4), the differences between the reference and land use scenario drain flow fractions, are very small and sporadic. The same is found for changes in recharge and groundwater head presented in Figure 7 and Figure 8 (top row). Averaged across the catchment, the change in land use gives rise to a maximum 1.2% change in reduction potential (Figure 4). For all 45 runs, the general statistics also show that changing the land use (horizontally, Table 4) does not change the mean reduction potential more than a maximum of  $\pm 2\%$ .

330

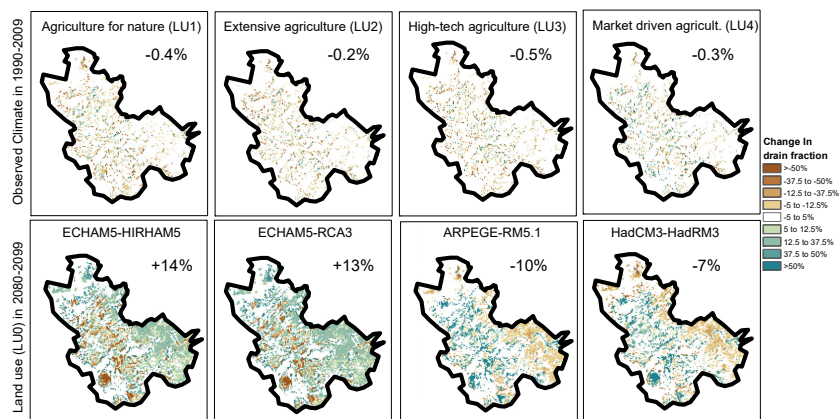


Figure 6: Changes in the drain flow fraction from baseline (LU0) to the four land use scenarios (LU1-4) in the observational period (top row) and from the reference period to the future period for four climate models using LU0 (bottom row). Drain flow fraction is defined as drain flow divided by net precipitation. Green colors indicate that a larger percentage of the net precipitation is channeled into the drains for the future. Number in upper right corner indicate the relative change in drain flow fraction from reference period to future period. The corresponding percentage of drain flow in the baseline scenario is 31%.

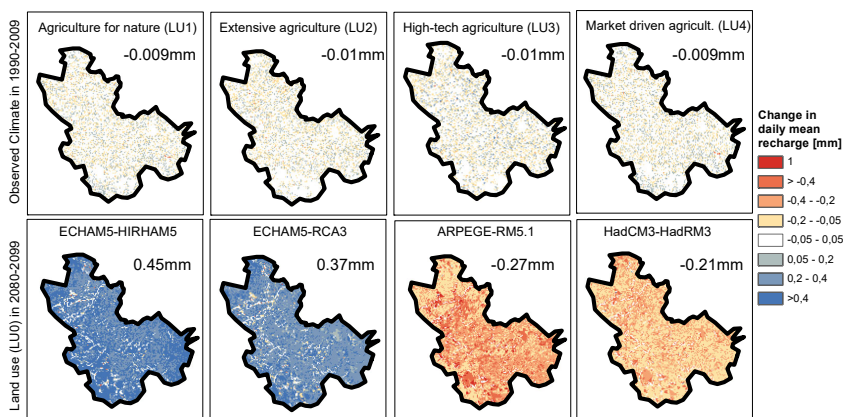
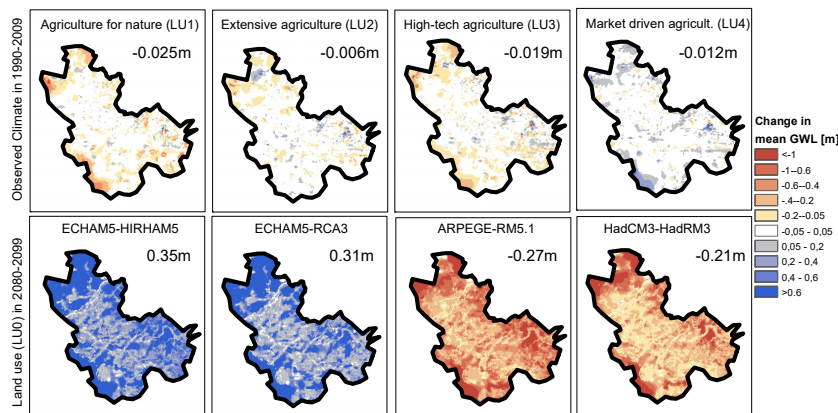


Figure 7: Changes in daily recharge from baseline (LU0) to the four land use scenarios (LU1-4) in the observational period (top row) and the change for four climate scenarios (LU0) from reference to future period (bottom row).



340



**Figure 8:** Changes in groundwater level from the upper saturated layer. Changes are reported as change from (LU0) to LU1-4 with observational climate for the top row and from RCM reference period to RCM future period for the bottom row. Figure modified from Karlsson et al. (2016).

#### 345 4.4 Impact of land use and climate change impact on reduction maps

Figure 4, bottom row, shows the results for the future climate compared to the corresponding reference period. For the future simulations, not only the water flow paths are affected by the change in amount and distribution of net precipitation, but also the vegetation uptake is considerably different increasing potential evapotranspiration. The impact of these changes is evaluated in Figure 5, right, where the changes in the flow components are shown from the reference to the future period. The climate model projections have important impacts on the distribution of the water balance components and substantial differences are found among the models. Even if land use remains constant, the timing and amount of nitrate leakage are subject to significant variations as a result of climate changes. For the reduction maps (Figure 4), these changes results in larger differences when compared to the maps produced for the reference period. Averaged across the catchment, changes of up to 7.3% point are recorded for the four scenarios and for all 45 scenarios the change is up to  $\pm 8\%$ .

355



From a water balance perspective, the four future climate model projections vary greatly, but may be grouped in two overall categories. The first category includes the wet models, ECHAM5-HIRHAM5 and ECHAM5-RCA3 (Table 1). Both show a small decrease in annual reference evapotranspiration. At the same time precipitation is projected to increase in all seasons resulting in an annual increase of 15 – 30%. As a result, the net precipitation (Figure 5) and groundwater recharge (Figure 7) increase considerably. Since there is a limit to how fast water can be pushed through the deeper groundwater systems, the fast flow components (overland, drain flow) both increase substantially.

Even though the drain flow produced with the wet climate model projections generally increases, the drain flow fraction, defined as the drain flow divided by net precipitation (Figure 6) shows two overall signals. In the eastern uphill area, the drain flow fractions are positive, while in the central and western areas, in the river valleys, the drain fraction is negative. This implies that less net precipitation, relatively, is channeled through the drainage system than in the reference period in the river valleys (brown areas), while relatively more net precipitation is captured by drains in the eastern uphill locations. This highlights how the change in the distribution of the flow components also changes the spatial pattern across the catchment. The underlying explanation for the pattern recognized in the wet models, is primarily found as a moderate increase in upwelling water to the drainage system in the lowlands in the future compared to the substantial increase in drainage in the uphill areas. The increase in groundwater recharge (Figure 7) results in increasing groundwater levels (Figure 8). However, the change varies across the catchment and since flow is controlled by the gradient in hydraulic head, the non-homogeneous changes in heads will result in changes in flow direction. The general tendency is that groundwater levels increase most in the upstream parts of the catchment, while it remains the same in the valleys near the stream. Hence, the gradients will become steeper, which results in an increase in the ratio of horizontal to vertical flow. Thus, this promotes near-surface flow paths in the subsurface.

As the fast flow components, like drain and overland flow, mainly carry non-reduced water, and the subsurface reduction depends on water being transported below the redox interface for nitrate reduction to take place, both the increase in fast flow



380 components and the shallower flow paths for the infiltrated water, is expected to give rise to a lower reduction potential as is indeed observed in Figure 4 and Table 4.

The second climate model category (dry models) includes ARPEGE-RM5.1 and HadCM3-HadRM3 (Table 1), that both show a significant increase in annual reference evapotranspiration of 10-20% (Karlsson et al., 2016). With respect to precipitation, 385 the two models show a slight decrease or no change in annual values, whereas lower precipitation is found during summer and autumn for both models. Therefore, net precipitation decreases for both models, leading to a decrease in the fast flow components (overland, drain flow) for the future projections (Figure 5). The reduction in net precipitation also results in a reversal of the distribution of the drain flow fraction (Figure 6) and a decreasing groundwater recharge (Figure 7).

390 These changes are reflected in the spatial distribution of the change in groundwater level (Figure 8). As found for the wet models, the general tendency is that groundwater levels change more in the upstream parts of the catchment compared to the valleys near the stream. Therefore, the gradients will become less steep, resulting in a decrease in the ratio of horizontal to vertical flow. This leads to a higher degree of slower and deeper groundwater flow paths, and potentially, to more nitrate crossing the redox interface.

395 The decrease in fast flow components and the deeper flow path supports the fact that the two models project higher reduction potential in the future. This is also found for one of the models, HadCM3-HadRM3, which generally has the largest increase in reduction potential of the four models, from the average reduction of 63% in the reference to 67% in the future simulation (LU0, Figure 4 and Table 4).

400 However, the other model, ARPEGE-RM5.1, shows a complete opposite signal with lower reduction potential (Figure 4). Initially, this anomaly did not seem to be explainable by changing flow paths as the changes (Figure 5, Figure 7 and Figure 8) are very similar to the other dry model. However, as mentioned previously, changes in the timing and quantities of the nitrate root zone leakage from Daisy is also a determining factor for the reduction map, and these dynamics are not always apparent



405 on average maps like the ones shown in Figure 4, Figure 5, Figure 7 and Figure 8. A closer inspection of the monthly changes  
in flow components and nitrate leakage provides a possible explanation for this phenomenon (calculations not shown).

The ARPEGE-RM5.1 model shows the absolute largest increase in nitrate leakage in January. Even though the model is  
generally dry, the January precipitation is projected to increase in the future. The dynamics in the model shows a shift in flow  
410 components for this month towards a smaller amount of drain flow and recharge, while overland flow increases, probably as  
a result of larger prolonged rainfall events. This shift combined with the very large increase in nitrate leakage leads to more  
non-reduced water in the system for the future period than for the control period. As this combination of larger nitrate leakage  
and flow components shifts are not seen in the HadCM3-HadRM3 model, it is, most likely, a result of the lower reduction  
potential for ARPEGE-RM5.1 in the future in spite of the overall drying signal from the model.

#### 415 **4.5 Effect on the nitrate flux using different reduction maps**

To evaluate the impacts of using a fixed reduction map versus different maps calculated for each scenario explicitly considering  
differences caused by changes in land use and climate change, the total catchment nitrate load (nitrate arrival at Kratholm)  
were calculated using two different approaches for all scenarios:

1. A fixed reduction map (the baseline reduction map) is used and combined with projected nitrate leaching from the  
420 root zone.
2. Targeted reduction maps, i.e. different reduction maps for each scenario (as calculated above) are used and  
combined with projected nitrate leaching from the root zone.

For both approaches nitrate arrival is calculated for the observational, reference and future periods. The resulting nitrate arrivals  
for approach 2 is then for each case compared to the corresponding scenario in approach 1; thereby illustrating the effect of  
425 using a targeted reduction map compared to a baseline reduction map (Figure 9).

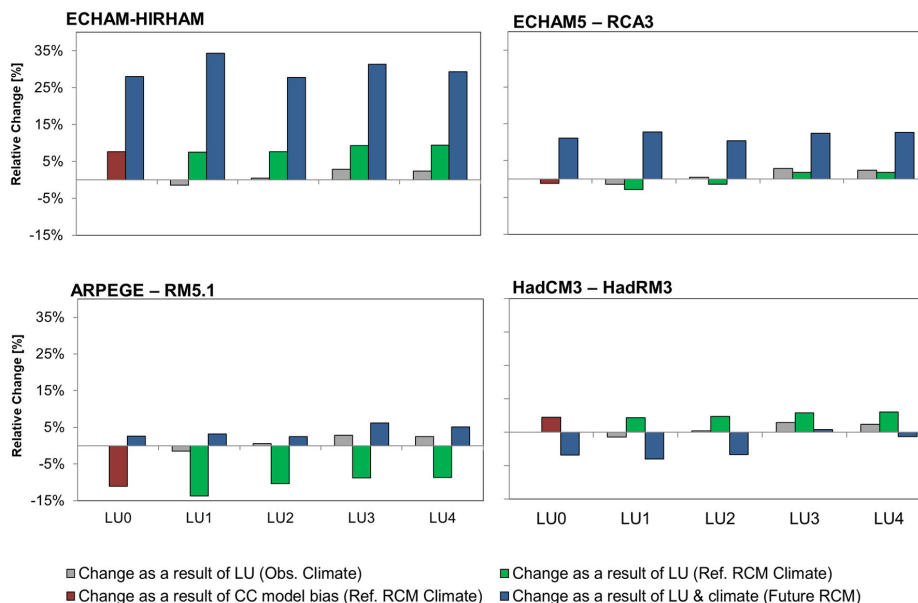


**Figure 9:** Bars denote the change in nitrate flux at the catchment outlet that arises from using either the baseline nitrate reduction potential map or the reduction map from the scenarios. The scenarios encompass cases with different land use (grey), climate model data for the present (red bar) with land use changes (green bars) or future climate data and land use changes (blue bars).

The grey bars in Figure 9 show the relative change (compared to baseline), when applying targeted reduction maps for the four land use scenarios, but using observed climate. Note therefore that the grey bars are the same for all four plots. The effect of the targeted reduction maps versus the fixed reduction map manifests in only limited spread in the estimated nitrate arrivals by only 1% - 3%. This implies that for a case of changing land use, the fixed reduction map is a reasonable approximation of the reduction potential in the catchment.

The green bars in Figure 9 represents the same effect as for the grey bars (targeted versus fixed reduction maps); however, here the climate is the reference climate for each of the four climate models. For all models, the effect is here larger than using the observed climate. This phenomenon is mainly due to the inherent bias of the reference climate model simulations. This





becomes clear when looking at the first bars of each plot (red bars), denoting the change when only observed climate is replaced by reference climate but maintaining the current land use setup (LU0). Even though the climate model output is bias corrected such that the general statistics in the reference period resembles those of the observations, there may still be differences in the temporal structure of the climate model outputs, which may impact hydrological simulations. This is an important issue to bear  
445 in mind when analyzing the future signal presented by the blue bars. However, the effect of land use can still be approximated by comparing the results from LU0 to LU1-4 for the different climate models. Again, the magnitude of the effect is between 1% - 3% change in nitrate arrival; however, the models do not agree on which land use causes the largest change (being either LU1 or LU4).

450 For the blue bars the differences from the fixed reduction map to targeted reduction maps become a combination of bias correction limitations, land use change and climate change. Even though it is not possible to completely separate the signal of these three components, a cautious estimation can again be achieved by comparing the blue bars to the results from LU0 in the reference period (red bars). For a dry model like ARPEGE-RM5.1 the effect (land use and climate) on the nitrate arrival is in the range of -5% to -9%, while for HadCM3-HadRM3, it is between -4% to 4%. The largest effects are found for the wet  
455 models, with changes ranging from 20% - 27% for ECHAM-HIRHAM, followed by ECHAM-RCA3 with 9% - 12%. This shows that the consequences of using a fixed reduction map may be considerable, in particular with large changes in climatic conditions.

## 5 Discussion and conclusions

### 460 5.1 N-reduction maps are not constant in time

Our analysis clearly demonstrates that N-reduction maps are a result of complicated interactions between climate, vegetation, geology and farm management leading to a diversity of potential nitrate inputs, distributions, timing, flow paths and reduction capability. This implies that N-reduction maps calculated for present climatic conditions and flow patterns will differ from N-reduction maps under future climate and land use conditions. The main factor causing this is differences in the



465 precipitation/evapotranspiration regime that results in differences in how large a fraction of the water percolating from the root zone reaches the stream via shallow flow routes above the redox interface, such as overland flow and runoff via drain pipes, and how large a fraction that takes a route through deeper groundwater zones and crosses the redox interface. Therefore, N-reduction maps also differ between a wet year and a dry year in the present climate.

470 Compared to climate effects, the impacts of land use change are minor, because land use change does not affect the flow regime to the same extent as variability and change in climate. This novel finding has not been recognized in previous studies of N-reduction maps such as Hansen et al. (2014b), Højberg et al. (2015), Andersen et al. (2016) and Refsgaard et al. (2019). Nevertheless, it is important to note that the distribution of drains in the catchment was not changed during the land use change scenarios. Hence, uniform drain distribution and parameterization are assumed, where the drainage component covers both  
475 natural (ditches and small canals) and agricultural drains. However, a different approach could have been adopted in the land use change scenarios by changing the drainage efficiency (by adjusting drainage parameters) in re- or deforested areas. Unfortunately, little information is available to guide this fine-tuning. However, the influence of land use change on the water balance and therefore the nitrate reduction is expected to increase if this effect is accounted for.

480 To encapsulate the full range of uncertainty and influences from climate and land use scenarios in this setup; all scenario combinations were used. However, it is also worth noting, that all combinations of land use and climate change scenarios may not be equally likely or even plausible in the future. This is because decisions on land use application made by local farmers or through national regulations are made concurrently to adapt or mitigate changes in the climatic conditions.

485 The present study was carried out for a groundwater dominated catchment characterized by till deposits, confined aquifers, and relatively shallow redox interfaces and phreatic groundwater tables. We consider the conclusions to be applicable to catchments with similar hydrogeological conditions, while they cannot be used in groundwater dominated catchments characterized by alluvial plains without fast flow components such as overland flow and drainpipe/ditch flow and aerobic groundwater systems without a redox-interface. Similarly, the conclusions cannot be transferred to surface water dominated



490 catchments, where the N-reduction takes place in streams and lakes, although we suspect that non-linearities may cause similar effects here.

In this study the location of redox interface was assumed to be the same for both present and future scenarios. While this assumption may be reasonable in relation to the slow natural migration of the redox interface caused by percolation of oxygen,  
495 the redox interface migration may be escalated by nitrate application on the land surface as reported by e.g. Böhlke et al. (2002) and Wriedt and Rode (2006). This issue cannot be addressed within the framework of this study, but the effect on the redox interface may be substantial especially for land use scenarios with high nitrate application.

## 5.2 Water management implications

The advantages of assuming a fixed reduction map is that any projected nitrate input, regardless of climate and land use  
500 scenario, can be multiplied with the reduction map and thus provide a projected nitrate outflow estimate with little effort and time spent. However, as is shown in the present study, the assumption that the reduction map is constant in a changing environment is problematic. The good question then is how large errors are made by assuming a fixed reduction map and how should this be dealt with in water management practices.

505 The analysis indicates that assuming fixed reduction maps leads to small errors when dealing with land use change impacts but may lead to substantial errors (up to 10% on catchment N load) when climate change projections are included. Land use change impacts may however be underestimated as a result of the uniform drainage setup. Whether such errors are acceptable depends on the purpose and context in specific water management situations. Thus, using fixed reduction maps may well be justifiable for initial screening purposes, while targeted reduction maps, explicitly calculated for specific scenarios, may be  
510 required for design of remediation measures having significant socio-economic impacts for stakeholders. Such effects should of course be seen in the context of the inherent uncertainties of the nitrate reduction maps (Hansen et al., 2014b).

The indication that errors can be up to 10% is based on only a single case study with one catchment, one model and a limited number of land use and climate change scenarios. The error will be site and context specific and therefore causes projection



515 uncertainties that should be addressed along with other known sources of uncertainty such as climate model projections, land  
use projections and hydrological model structural uncertainty (Karlsson et al., 2016).

#### **Author contributions**

IKS performed model simulations, wrote part of the paper and produced figures. TSO and JCR contributed to formulation of  
the conceptualization, methodology and simulation assistance, as well as the writing of the paper. DT, CDB and JEO  
520 contributed to the methodology and the writing of the paper. CDB and JEO additionally provided input data and results for the  
paper.

#### **Competing interests.**

The authors declare that they have no conflict of interest.

#### 525 **Data/code availability**

The hydrological model is based on the commercial software MIKE SHE and therefore model code is not available.

Data from the study is available upon request and through the public server at <https://dataverse01.geus.dk>. An exception to  
this is the climate data input which is owned by the Danish Meteorological Institute (DMI).

#### 530 **Acknowledgements**

The present study was funded by a grant from the Danish Strategic Research Council for the Centre for Regional Change in  
the Earth System (CRES – [www.cres-centre.dk](http://www.cres-centre.dk)) under contract no: DSF-EnMi 09-066868.

#### **References**

- Abbott, M. B., Bathurst, J. C., Cunge, J. A., O'Connell, P. E., and Rasmussen, J.: An introduction to the European hydrological  
535 system – système hydrologique européen, “She”, 2: Structure of a physically-based, distributed modeling system, *Journal of  
Hydrology*, 87, 61-77, 1986.
- Abrahamsen, P., and Hansen, S.: Daisy: an open soil-crop-atmosphere system model, *Environmental modelling & software*,  
15, 313-330, 2000.



- Allen, R. G., Pereira, L. S., Raes, D., and Smith, M.: Crop evapotranspiration - Guidelines for computing crop water requirements, FAO - Food and Agriculture Organization of the United Nations, Rome, Italy, 333, 1998.
- 540 Andersen, H. E., Blicher-Mathiesen, G., Thodsen, H., Andersen, P. M., Larsen, S. E., Stålnacke, P., Humborg, C., Mörth, C.-M., and Smedberg, E.: Identifying Hot Spots of Agricultural Nitrogen Loss Within the Baltic Sea Drainage Basin, *Water, Air, & Soil Pollution*, 227, 38, 10.1007/s11270-015-2733-7, 2016.
- Böhlke, J. K., Wanty, R., Tuttle, M., Delin, G., and Landon, M.: Denitrification in the recharge area and discharge area of a  
545 transient agricultural nitrate plume in a glacial outwash sand aquifer, Minnesota, *Water Resources Research*, 38, 10-11-10-26, 10.1029/2001WR000663, 2002.
- Børgesen, C. D., and Olesen, J. E.: A probabilistic assessment of climate change impacts on yield and nitrogen leaching from winter wheat in Denmark, *Natural Hazards and Earth System Sciences*, 11, 2541-2553, 10.5194/nhess-11-2541-2011, 2011.
- Børgesen, C. D., Jensen, P. N., Blicher-Mathiesen, G., Schelde, K., Grant, R., Vinther, F. P., Thomsen, I. K., Hansen, E. M.,  
550 Kristensen, I. T., Sørensen, P., and Poulsen, H. D.: Udviklingen i kvælstofudvaskning of næringsstofoverskud fra dansk landbrug for perioden 2007-2011. Evaluering af implementerede virkemidler til reduktion af kvælstofudvaskning samt en fremskrivning af planlagte virkemidlers effekt frem til 2015, DCA - Nationalt Center for Fødevarer og Jordbrug, Tjele, Denmark, 2013.
- DHI: User Guide, DHI – Water & Environment, Hørsholm, Denmark, 2019.
- 555 Diaz, R. J., and Rosenberg, R.: Spreading dead zones and consequences for marine ecosystems, *Science*, 321, 926-929, 10.1126/science.1156401, 2008.
- Ernstsen, V., Koch, J., and Højberg, A. L.: Dybden til redoxgrænsen, 100 m grid. (GEUS), D. N. G. U. f. D. o. G. (Ed.), Copenhagen, GEUS, 2019.
- Ernstsen, V. H., A.L., Jakobsen, P.R., von Platen,, F., T., L, Hansen, J.R., Blicher-Mathiasen, G.,, and Bøgestrand, J., Børgesen,  
560 C.D., : Beregning af nitratreduktionsfaktorer for zonen mellem rodzonen og frem til vandløbet. Data og metode for 1. generationskortet. , Danmarks og Grønlands Geologiske Undersøgelse, Copenhagen, Denmark, 2006.
- Graham, D. N., and Butts, M. B.: Flexible, integrated watershed modelling with MIKE SHE, in: *Watershed Models*, edited by: Singh, V. P., and Frevert, D. K., 245-272, 2005.
- Greve, M. H., Greve, M. B., Bøcher, P. K., Balstrøm, T., Madsen, H. B., and Krogh, L.: Generating a Danish raster-based  
565 topsoil property map combining choropleth maps and point information, *Geografisk Tidsskrift*, 107, 2007.
- Hansen, A. L., Christensen, B. S. B., Ernstsen, V., He, X., and Refsgaard, J. C.: A concept for estimating depth of the redox interface for catchment-scale nitrate modelling in a till area in Denmark, *Hydrogeology Journal*, 22, 1639-1655, 10.1007/s10040-014-1152-y, 2014a.
- Hansen, A. L., Gunderman, D., He, X., and Refsgaard, J. C.: Uncertainty assessment of spatially distributed nitrate reduction  
570 potential in groundwater using multiple geological realizations, *Journal of Hydrology*, 519, Part A, 225-237, <http://dx.doi.org/10.1016/j.jhydrol.2014.07.013>, 2014b.



- Hansen, A. L., Refsgaard, J. C., Olesen, J. E., and Børgesen, C. D.: Potential benefits of a spatially targeted regulation based on detailed N-reduction maps to decrease N-load from agriculture in a small groundwater dominated catchment, *Science of The Total Environment*, 595, 325-336, <https://doi.org/10.1016/j.scitotenv.2017.03.114>, 2017.
- 575 Hansen, B., Dalgaard, T., Thorling, L., and Sørensen, B.: Regional analysis of groundwater nitrate concentrations and trends in Denmark in regard to agricultural influence, *Biogeosciences Discussions*, 10.5194/bgd-9-5321-2012, 2012.
- Hansen, S., Jensen, H. E., Nielsen, N. E., and Svendsen, H.: Simulation of nitrogen dynamics and biomass production in winter wheat using the Danish simulation model DAISY, *Fertilizer Research*, 27, 245-259, 10.1007/BF01051131, 1991.
- Højberg, A. L., J. W., CD, B., L. T., H. T., G. B.-M., B. K., and H. T.: En ny kvælstofmodel. Oplandsmodel til belastning og virkemidler. Metode rapport (A new nitrogen model. Catchment model for loads and measures. Methodology Report – In Danish), 2015.
- 580 Karlsson, I. B., Sonnenborg, T. O., Seaby, L. P., Jensen, K. H., and Refsgaard, J. C.: The climate change impact of a high-end CO<sub>2</sub>-emission scenario on hydrology, *Climate Research*, doi: 10.3354/cr01265, 2015.
- Karlsson, I. B., Sonnenborg, T. O., Refsgaard, J. C., Trolle, D., Børgesen, C. D., Olesen, J. E., Jeppesen, E., and Jensen, K. H.: Combined effects of climate models, hydrological model structures and land use scenarios on hydrological impacts of climate change, *Journal of Hydrology*, 535, 301-317, <http://dx.doi.org/10.1016/j.jhydrol.2016.01.069>, 2016.
- Koch, J., Stisen, S., Refsgaard, J. C., Ernstsén, V., Jakobsen, P. R., and Højberg, A. L.: Modeling Depth of the Redox Interface at High Resolution at National Scale Using Random Forest and Residual Gaussian Simulation, 55, 1451-1469, 10.1029/2018wr023939, 2019.
- 590 Kristensen, K. J., and Jensen, S. E.: A Model for Estimating Actual Evapotranspiration from Potential Evapotranspiration, *Hydrology Research*, 6, 170-188, 1975.
- Madsen, H.: Automatic calibration of a conceptual rainfall-runoff model using multiple objectives, *Journal of Hydrology*, 235, 276-288, 10.1016/S0022-1694(00)00279-1, 2000.
- Møller, J., Thøgersen, R., Helleshøj, M. E., Weisbjerg, M. R., Søgaard, K., and Hvelplund, T.: Fodermiddeltabel - Sammensætning og foderværdi af fodermidler til kvæg, 64, 2005.
- 595 Olesen, J. E., Jeppesen, E., Porter, J. R., Børgesen, C. D., Trolle, D., Refsgaard, J. C., Sonnenborg, T., and Karlsson, I. B.: Scenarier for fremtidens arealanvendelse i Danmark, *Vand og Jord*, 21, 126-129, 2014.
- Olesen, J. E., Børgesen, C. D., Hashemi, F., Jabloun, M., Bar-Michalczyk, D., Wachniew, P., Zurek, A. J., Bartosova, A., Bosshard, T., Hansen, A. L., and Refsgaard, J. C.: Nitrate leaching losses from two Baltic Sea catchments under scenarios of changes in land use, land management and climate, *Ambio*, 48, 1252-1263, 10.1007/s13280-019-01254-2, 2019.
- 600 Postma, D., Boesen, C., Kristiansen, H., and Larsen, F.: Nitrate Reduction in an Unconfined Sandy Aquifer: Water Chemistry, Reduction Processes, and Geochemical Modeling, *Water Resources Research*, 27, 2027-2045, 10.1029/91wr00989, 1991.
- Refsgaard, J. C., Hansen, A. L., Højberg, A. L., Olesen, J. E., Hashemi, F., Wachniew, P., Wörman, A., Bartosova, A., Stelljes, N., and Chubarenko, B.: Spatially differentiated regulation: Can it save the Baltic Sea from excessive N-loads?, *Ambio*, 48, 1278-1289, 10.1007/s13280-019-01195-w, 2019.
- 605



- Reusch, T. B. H., Dierking, J., Andersson, H. C., Bonsdorff, E., Carstensen, J., Casini, M., Czajkowski, M., Hasler, B., Hinsby, K., Hyytiäinen, K., Johannesson, K., Jomaa, S., Jormalainen, V., Kuosa, H., Kurland, S., Laikre, L., MacKenzie, B. R., Margonski, P., Melzner, F., Oesterwind, D., Ojaveer, H., Refsgaard, J. C., Sandström, A., Schwarz, G., Tonderski, K., Winder, M., and Zandersen, M.: The Baltic Sea as a time machine for the future coastal ocean, *Science Advances*, 4, eaar8195, 10.1126/sciadv.aar8195, 2018.
- 610 Seaby, L. P., Refsgaard, J. C., Sonnenborg, T. O., Stisen, S., Christensen, J. H., and Jensen, K. H.: Assessment of robustness and significance of climate change signals for an ensemble of distribution-based scaled climate projections, *Journal of Hydrology*, 486, 479–493, 2013.
- Statistikbanken: Statistical regional registered annual mean yields. (In Danish) <https://www.statistikbanken.dk/jord3>, 2015.
- 615 Styczen, M., Hansen, S., Jensen, L. S., Svendsen, H., Abrahamsen, P., Børgesen, C. D., Thirup, C., and Østergaard, H. S.: Standardopstillinger til Daisy-modellen. Vejledning og baggrund, Institut for Vand og Miljø, DHI, 62, 2004.
- Trolle, D., Nielsen, A., Andersen, H. E., Thodsen, H., Olesen, J. E., Børgesen, C. D., Refsgaard, J. C., Sonnenborg, T. O., Karlsson, I. B., Christensen, J. P., Markager, S., and Jeppesen, E.: Effects of changes in land use and climate on aquatic ecosystems: Coupling of models and decomposition of uncertainties, *Science of The Total Environment*, 657, 627-633, <https://doi.org/10.1016/j.scitotenv.2018.12.055>, 2019.
- 620 van Genuchten, M. T.: A Closed-form Equation for Predicting the Hydraulic Conductivity of Unsaturated Soils, 44, 892-898, 10.2136/sssaj1980.03615995004400050002x, 1980.
- Wriedt, G., and Rode, M.: Modelling nitrate transport and turnover in a lowland catchment system, *Journal of Hydrology*, 328, 157-176, <http://dx.doi.org/10.1016/j.jhydrol.2005.12.017>, 2006.
- 625
- Abbott, M.B., Bathurst, J.C., Cunge, J.A., O’Connell, P.E., Rasmussen, J., 1986. An introduction to the European hydrological system – système hydrologique européen, “She”, 2: Structure of a physically-based, distributed modeling system. *Journal of Hydrology*, 87: 61-77.
- 630 Abrahamsen, P., Hansen, S., 2000. Daisy: an open soil-crop-atmosphere system model. *Environmental modelling & software*, 15(3): 313-330.
- Allen, R.G., Pereira, L.S., Raes, D., Smith, M., 1998. Crop evapotranspiration - Guidelines for computing crop water requirements, FAO - Food and Agriculture Organization of the United Nations, Rome, Italy.
- Andersen, H.E. et al., 2016. Identifying Hot Spots of Agricultural Nitrogen Loss Within the Baltic Sea Drainage Basin. *Water, Air, & Soil Pollution*, 227(1): 38. DOI:10.1007/s11270-015-2733-7
- 635 Böhlke, J.K., Wanty, R., Tuttle, M., Delin, G., Landon, M., 2002. Denitrification in the recharge area and discharge area of a transient agricultural nitrate plume in a glacial outwash sand aquifer, Minnesota. *Water Resources Research*, 38(7): 10-1-10-26. DOI:10.1029/2001WR000663
- Børgesen, C.D. et al., 2013. Udviklingen i kvælstofudvaskning af næringsstofferskud fra dansk landbrug for perioden 2007-2011. Evaluering af implementerede virkemidler til reduktion af kvælstofudvaskning samt en fremskrivning af planlagte virkemidlers effekt frem til 2015, DCA - Nationalt Center for Fødevarer og Jordbrug, Tjele, Denmark.
- 640 Børgesen, C.D., Olesen, J.E., 2011. A probabilistic assessment of climate change impacts on yield and nitrogen leaching from winter wheat in Denmark. *Natural Hazards and Earth System Sciences*, 11(9): 2541-2553. DOI:10.5194/nhess-11-2541-2011
- 645 DHI, 2019. User Guide, DHI – Water & Environment, Hørsholm, Denmark.



- Diaz, R.J., Rosenberg, R., 2008. Spreading dead zones and consequences for marine ecosystems. *Science*, 321(5891): 926-9. DOI:10.1126/science.1156401
- Ernstsen, V., Koch, J., Højberg, A.L., 2019. Dybden til redoxgrænsen, 100 m grid. In: (GEUS), D.N.G.U.f.D.o.G. (Ed.), Copenhagen, GEUS.
- 650 DOI:[https://data.geus.dk/geusmap/?mapname=denmark#baslay=baseMapDa&optlay=&extent=-139925.69284407864,5929490.944444444,1254925.6928440786,6520509.055555556&layers=redox\\_dybd\\_100m\\_grid](https://data.geus.dk/geusmap/?mapname=denmark#baslay=baseMapDa&optlay=&extent=-139925.69284407864,5929490.944444444,1254925.6928440786,6520509.055555556&layers=redox_dybd_100m_grid)
- Ernstsen, V.H., A.L., Jakobsen, P.R., von Platen, F., T., L., Hansen, J.R., Blicher-Mathiasen, G., Bøgestrand, J., Børgesen, C.D., , 2006. Beregning af nitratreduktionsfaktorer for zonen mellem rodzonen og frem til vandløbet. Data og metode for 1. generationskortet. , Danmarks og Grønlands Geologiske Undersøgelse, Copenhagen, Denmark.
- 655 Graham, D.N., Butts, M.B., 2005. Flexible, integrated watershed modelling with MIKE SHE. In: Singh, V.P., Frevert, D.K. (Eds.), *Watershed Models*, pp. 245-272.
- Greve, M.H. et al., 2007. Generating a Danish raster-based topsoil property map combining choropleth maps and point information. *Geografisk Tidsskrift*, 107.
- 660 Hansen, A.L., Christensen, B.S.B., Ernstsen, V., He, X., Refsgaard, J.C., 2014a. A concept for estimating depth of the redox interface for catchment-scale nitrate modelling in a till area in Denmark. *Hydrogeology Journal*, 22(7): 1639-1655. DOI:10.1007/s10040-014-1152-y
- Hansen, A.L., Gunderman, D., He, X., Refsgaard, J.C., 2014b. Uncertainty assessment of spatially distributed nitrate reduction potential in groundwater using multiple geological realizations. *Journal of Hydrology*, 519, Part A: 225-237. DOI:<http://dx.doi.org/10.1016/j.jhydrol.2014.07.013>
- 665 Hansen, A.L., Refsgaard, J.C., Olesen, J.E., Børgesen, C.D., 2017. Potential benefits of a spatially targeted regulation based on detailed N-reduction maps to decrease N-load from agriculture in a small groundwater dominated catchment. *Science of The Total Environment*, 595: 325-336. DOI:<https://doi.org/10.1016/j.scitotenv.2017.03.114>
- Hansen, B., Dalgaard, T., Thorling, L., Sørensen, B., 2012. Regional analysis of groundwater nitrate concentrations and trends in Denmark in regard to agricultural influence. *Biogeosciences Discussions*. DOI:10.5194/bgd-9-5321-2012
- 670 Hansen, S., Jensen, H.E., Nielsen, N.E., Svendsen, H., 1991. Simulation of nitrogen dynamics and biomass production in winter wheat using the Danish simulation model DAISY. *Fertilizer Research*, 27(2-3): 245-259. DOI:10.1007/BF01051131
- Højberg, A.L. et al., 2017. Review and assessment of nitrate reduction in groundwater in the Baltic Sea Basin. *Journal of Hydrology: Regional Studies*, 12: 50-68. DOI:<https://doi.org/10.1016/j.ejrh.2017.04.001>
- 675 Højberg, A.L. et al., 2015. En ny kvælstofmodel. Oplandsmodel til belastning og virkemidler. Metode rapport (A new nitrogen model. Catchment model for loads and measures. Methodology Report – In Danish). DOI:Available from [http://www.geus.dk/DK/water-soil/water-cycle/Documents/national\\_kvaelstofmodel\\_metoderapport.pdf](http://www.geus.dk/DK/water-soil/water-cycle/Documents/national_kvaelstofmodel_metoderapport.pdf)
- Karlsson, I.B. et al., 2014. Significance of hydrological model choice and land use changes when doing climate change impact assessment. In: EGU (Ed.), EGU General Assembly 2014. *Geophysical Research Abstracts*, Vienna, Austria, pp. 1.
- 680 Karlsson, I.B. et al., 2016. Combined effects of climate models, hydrological model structures and land use scenarios on hydrological impacts of climate change. *Journal of Hydrology*, 535: 301-317. DOI:<http://dx.doi.org/10.1016/j.jhydrol.2016.01.069>
- 685 Karlsson, I.B., Sonnenborg, T.O., Seaby, L.P., Jensen, K.H., Refsgaard, J.C., 2015. The climate change impact of a high-end CO2-emission scenario on hydrology. *Climate Research*. DOI:doi: 10.3354/cr01265
- Koch, J. et al., 2019. Modeling Depth of the Redox Interface at High Resolution at National Scale Using Random Forest and Residual Gaussian Simulation. 55(2): 1451-1469. DOI:10.1029/2018wr023939
- Kristensen, K.J., Jensen, S.E., 1975. A Model for Estimating Actual Evapotranspiration from Potential Evapotranspiration. *Hydrology Research*, 6: 170-188.
- 690 Kunkel, R., Eisele, M., Schäfer, W., Tetzlaff, B., Wendland, F., 2008. Planning and implementation of nitrogen reduction measures in catchment areas based on a determination and ranking of target areas. *Desalination*, 226(1): 1-12. DOI:<https://doi.org/10.1016/j.desal.2007.01.231>
- Madsen, H., 2000. Automatic calibration of a conceptual rainfall-runoff model using multiple objectives. *Journal of Hydrology*, 235: 276-288. DOI:10.1016/S0022-1694(00)00279-1
- 695





- Merz, C., Steidl, J., Dannowski, R., 2009. Parameterization and regionalization of redox based denitrification for GIS-  
embedded nitrate transport modeling in Pleistocene aquifer systems. *Environ Geol*, 58(7): 1587-1599.  
DOI:10.1007/s00254-008-1665-6
- Møller, J. et al., 2005. Fodermiddeltabel - Sammensætning og foderværdi af fodermidler til kvæg. 64.
- 700 Olesen, J.E. et al., 2019. Nitrate leaching losses from two Baltic Sea catchments under scenarios of changes in land use, land  
management and climate. *Ambio*, 48(11): 1252-1263. DOI:10.1007/s13280-019-01254-2
- Olesen, J.E. et al., 2014. Scenarier for fremtidens arealanvendelse i Danmark. *Vand og Jord*, 21(3): 126-129.
- Postma, D., Boesen, C., Kristiansen, H., Larsen, F., 1991. Nitrate Reduction in an Unconfined Sandy Aquifer: Water  
Chemistry, Reduction Processes, and Geochemical Modeling. *Water Resources Research*, 27(8): 2027-2045.  
705 DOI:10.1029/91wr00989
- Refsgaard, J.C. et al., 2019. Spatially differentiated regulation: Can it save the Baltic Sea from excessive N-loads? *Ambio*,  
48(11): 1278-1289. DOI:10.1007/s13280-019-01195-w
- Reusch, T.B.H. et al., 2018. The Baltic Sea as a time machine for the future coastal ocean. *Science Advances*, 4(5):  
eaar8195. DOI:10.1126/sciadv.aar8195
- 710 Seaby, L.P. et al., 2013. Assessment of robustness and significance of climate change signals for an ensemble of distribution-  
based scaled climate projections. *Journal of Hydrology*, 486: 479-493.
- Statistikbanken, 2015. Statistical regional registered annual mean yields. (In Danish) <https://www.statistikbanken.dk/jord3>.
- Styczen, M. et al., 2004. Standardopstillinger til Daisy-modellen. Vejledning og baggrund, Institut for Vand og Miljø, DHI.
- Trolle, D. et al., 2019. Effects of changes in land use and climate on aquatic ecosystems: Coupling of models and  
715 decomposition of uncertainties. *Science of The Total Environment*, 657: 627-633.  
DOI:<https://doi.org/10.1016/j.scitotenv.2018.12.055>
- van Genuchten, M.T., 1980. A Closed-form Equation for Predicting the Hydraulic Conductivity of Unsaturated Soils. 44(5):  
892-898. DOI:10.2136/sssaj1980.03615995004400050002x
- van Vuuren, D.P. et al., 2011. The representative concentration pathways: an overview. *Climatic Change*, 109(1): 5.  
720 DOI:10.1007/s10584-011-0148-z
- Wriedt, G., Rode, M., 2006. Modelling nitrate transport and turnover in a lowland catchment system. *Journal of Hydrology*,  
328(1-2): 157-176. DOI:<http://dx.doi.org/10.1016/j.jhydrol.2005.12.017>
- Wulff, F. et al., 2014. Reduction of Baltic Sea Nutrient Inputs and Allocation of Abatement Costs Within the Baltic Sea  
Catchment. *AMBIO*, 43(1): 11-25. DOI:10.1007/s13280-013-0484-5
- 725